

# High Voltage Gain Boost Converter for Micro source Power Conversion system

K. Radhalakshmi<sup>1</sup>, R. Dhanasekaran<sup>2</sup>

<sup>1</sup>Sethu Institute of Technology/EEE, Pulloor, Kariapatti, Tamil Nadu, India  
rajradha7981@gmail.com

<sup>2</sup>Syed Ammal Engineering College/Research-Director, Ramanathapuram, India  
rdhanashekar@yahoo.com

**Abstract**— In this paper, a new boost converter is introduced. In the proposed converter, a coupled inductor and voltage lift technique is used for raising the voltage gain. The designed converter especially for large voltage conversion ratio applications. By combining coupled inductor and voltage lift technique, the energy stored in the leakage inductor is recycled, therefore reduce the switch turn-off voltage and implement soft switching turn-on operation. The operating principles and steady-state analyses of continuous-conduction mode is discussed in detail. A 250W Converter Operating at 50KHZ with 25V input and 240V output simulation is presented to demonstrate the performance.

**Index Terms**—Boost Converter, Coupled Inductor, Voltage Lift Technique, High Voltage Gain

## I. INTRODUCTION

In recent Years, renewable energy is becoming increasingly important in distribution System, which provide different choice to electricity consumers whether they receive power from the main electricity source or in forming a micro source not only to fulfill their own demand but alternatively to be a power producer supplying a microgrid.

A microgrid usually includes various microsources and loads. Microsource categories are comprised of diverse renewable energy applications, Such as solar cell modules and fuel cell stacks. Fig.1. Shows a regular schematic of a microgrid unit supplied by various microsources; the boost converter is used to increase the output voltage of the microsource from 230-250V for the dc interface to the main electricity source through the dc-ac inverter [1],[2],[3]. Both the single solar cell module and the fuel cell stacks are low-voltage sources, thus a high step-up voltage gain dc-dc converter is required to regulate the voltage of the dc-dc interface.

The conventional Boost converters cannot provide such a high dc voltage gain, even for an extreme duty cycle. It also may results in serious reverse-recovery problems and increases the rating of all devices. As a result, the conversion efficiency is degraded and the electromagnetic interference (EMI) problem is severe under this situation [4]. In order to increase the conversion efficiency and voltage gain, many modified boost converter topologies have been investigated in the past decade [5]-[18].

Two winding coupled inductor is used and voltage gain is limited by turn ratio of transformer [5],[6]. The Buck-Boost type converter operated in a duty ratio is higher than 0.5, high

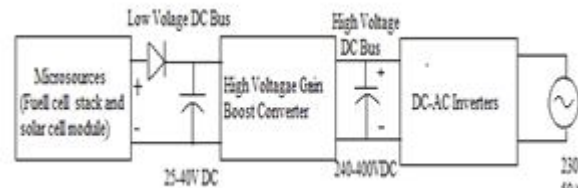


Figure 1. general Power Conversion System with a High Voltage Gain Boost Converter

voltage stresses on converter switches [7]. The presented Converters in are used for fuel cell power conversion systems [8],[9],[10]. The operation of the main switch is hard switching so turn on switching loss is high, this does not improve the efficiency sufficiently [8]. In practical situation, the maximum output voltage will be affected by parasitic effects, such as winding resistances of inductors, so the conversion ratio can be decreased [9]. In [10], the active switch can suffer with very high current during the switch on period and this converter is suitable for low to middle power applications. A zero-voltage switching dc-dc converter with high voltage gain [11] consists of a ZVS boost converter stage and a ZVS half-bridge converter stage. The efficiency of the converter at light load is lower due to the additional conduction loss of the auxiliary circuit of the ZVS boost converter stage. In [12], the cascaded high step-up dc-dc converter with single switch is low efficiency converter is up to 92% at 30% full load. If low input voltage applied in dc-dc converter [13], it experiences extremely high input current at full load and high conduction loss during the switch turn-on period. The bidirectional zero voltage switching dc-dc converter [14], efficiency is improved at heavy load. The conduction loss due to auxiliary circuit causes the relatively low efficiency at light load. In [15] the converter is a fixed frequency ZVS current fed converter that uses a very simple auxiliary circuit to create ZVS over an extended range of load. However the main converter switches and active clamp switch have significant amount of conduction losses, since current flows either through the active clamp switch. The overlap of voltage and current in the bridge switches when they turn off creates considerable losses when the converter operating under heavy load conditions. The several conventional converters are presented with active clamp, snubber, voltage multiplier and coupled inductor [16], [17], [18]. Soft Switching boost converter [16] is used to reduce current and voltage stress of the main switch. To achieve both soft switching features, more component count is usually required.

This paper presents a high voltage gain Boost Converter, which uses the coupling inductor and voltage lift technique. The circuit diagram of proposed converter is shown in fig.2. and the features of this converter are as follows: 1) High Voltage gain 2) Duty ratio can be designed to 0.65 by adjusting the turns ratio of the coupled inductor. Thus the converter can be operated under Continuous conduction mode. 3) The energy stored in the leakage inductance of the transformer is recycled, thus increasing the efficiency. 4) The voltage is

clamped on the active switch, enabling the power switch to be selected with a low voltage rating and low conduction resistance  $r_{ds}$ . 5) The converter uses low-rating switch and diodes to minimize the cost.

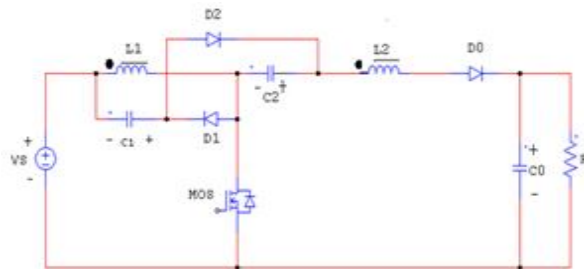


Figure 2. Circuit Diagram of High Voltage Gain Boost Converter

## II. PROPOSED CONVERTER AND OPERATION PRINCIPLE

Fig.3. Shows circuit configuration of the proposed converter, which is a boost converter with voltage lift technique and a coupled inductor. The equivalent model of the coupled inductor includes the magnetizing inductor  $L_m$ , leakage inductors  $L_{K1}$  and  $L_{K2}$  and an ideal transformer. This converter consists of a DC input voltage  $V_{in}$ , one power switch, one coupled inductor, three diodes and three capacitors. The boost converter is adopted to generate a stable voltage  $V_{C1}$  and to supply the energy for the load. Additionally, the diode  $D1$  is turned on when switch  $S$  is in turned-off period, the voltage across switch  $S$  is clamped at a low voltage level, and the energy stored in the leakage inductance is recycled into  $C1$ . Since switch  $S$  has a low voltage rating and low conduction resistance  $r_{ds(on)}$ , the proposed converter has high efficiency. The voltage-lift technique is applied to generate a constant voltage  $V_{C2}$  and provide the energy to output. Because the voltage across  $C2$  is constant, the voltage gain can be enhanced. Furthermore, the turn ratio of the coupled inductor is adjusted to achieve a high step-up voltage gain.

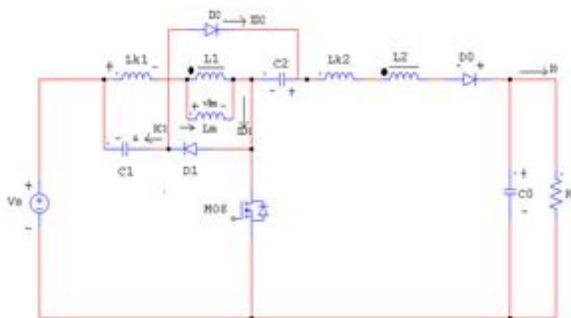


Figure 3. Circuit configuration of Proposed Converter

To simplify the circuit analysis, the following conditions are assumed:

1. Capacitors  $C1$ ,  $C2$  and  $C0$  are large enough that the  $V_{C1}$ ,  $V_{C2}$ , and  $V0$  are constant values in one switching period.
2. All semiconductor components are ideal.
3. Most of the energy is stored in the magnetizing inductance  $L_m$ , which is larger than the leakage inductance  $L_{K1}$  and  $L_{K2}$ .
4. Turns ratio of the coupled inductor  $n = N_2/N_1$ .

### A. Continuous Conduction Mode

The Proposed converter operating in continuous conduction mode is analyzed. Fig.4. illustrates some typical waveforms under CCM operation in one switching period. The operating principle of CCM is divided into six modes during each switching period. The operating modes are described as follows:

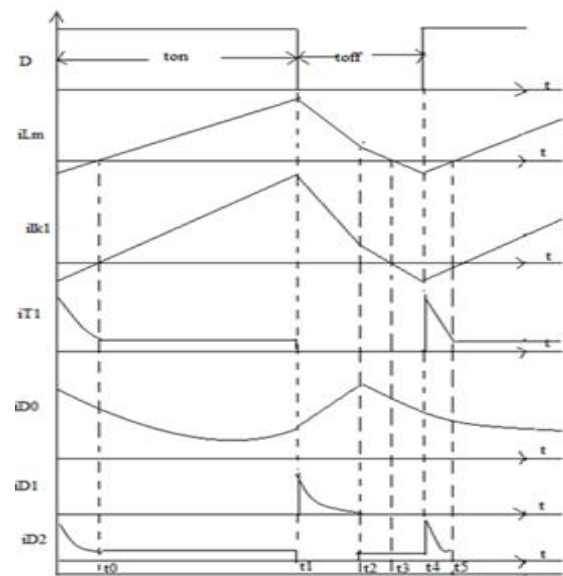
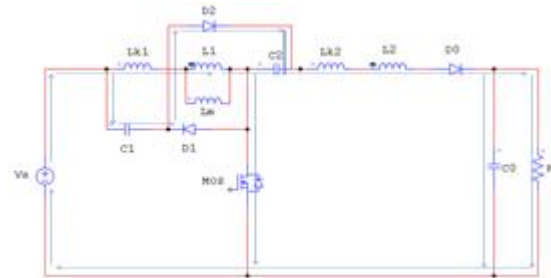
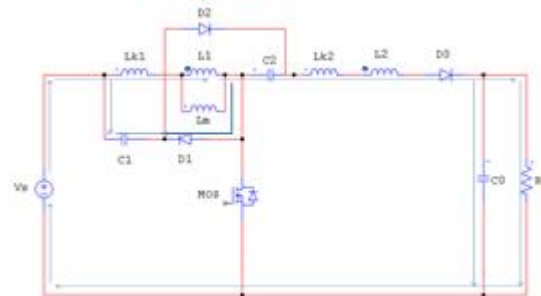


Figure 4. Some typical waveforms under CCM operation



(a) Mode 1  $[t_0-t_1]$



(b) Mode 2  $[t_1-t_2]$

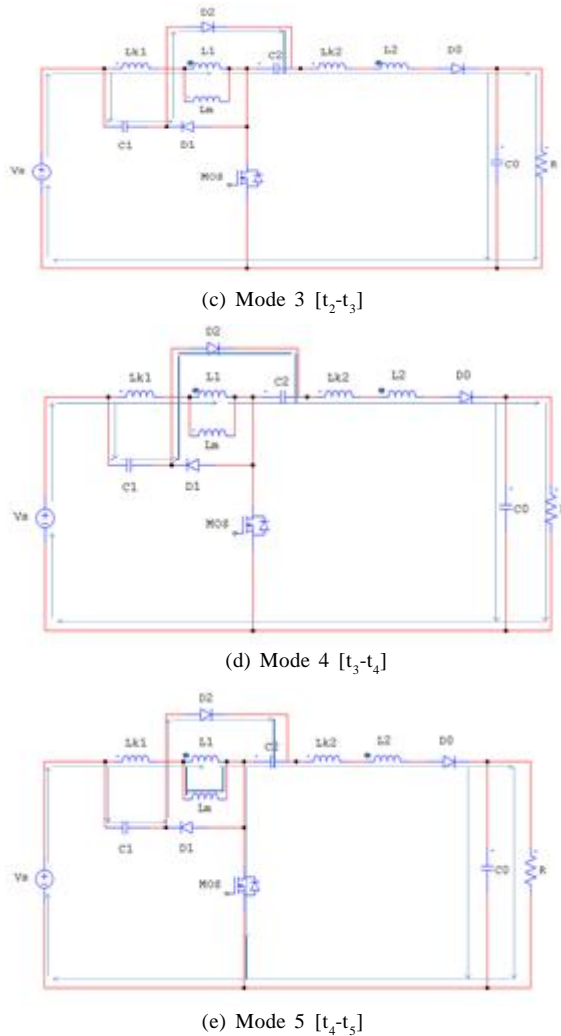


Figure 5. Operating modes for CCM

**(a). Mode 1  $[t_0-t_1]$** 

In this mode, the switch Q was turned on for a span. The magnetizing inductor ( $L_m$ ) is charged by the input voltage source ( $V_s$ ), the magnetizing current ( $i_{lm}$ ) increases gradually in an approximately linear way. The secondary voltage ( $V_{l2}$ ) is charged the capacitor  $C_2$  through the switch (Q). At  $t=t_0$ , the switch S is turned on, diodes  $D_2$  and  $D_3$  are turned on and  $D_1$  is turned off. Fig.5. (a) shows the equivalent circuit of the proposed converter in this mode.

**(b). Mode 2  $[t_1-t_2]$** 

At  $t=t_1$ , switch Q is turned off, the voltage across the switch  $V_{DS}=V_s+V_{C1}$ . Switch Q and diode  $D_2$  is turned off without reverse recovery current and diode  $D_1$  is turned on. During this period, the energy stored in inductor released to the output terminal the current through the output diode  $D_o$  increased and current through the leakage inductor is reduced. The equivalent circuit of proposed converter of this mode is shown in Fig.5. (b).

**(c). Mode 3  $[t_2-t_3]$** 

At  $t=t_2$ , S is still turned off. At this time interval, the current through the leakage inductor  $L_{k1}$  and  $L_m$  are decays to zero. Diode  $D_1$  is turned off and Diode  $D_2$  is turned on. Fig.5. (c)

Shows the equivalent circuit of this mode. In this mode the circuit current flows is still directed to the output terminal, but the magnitudes of current decreases gradually.

**(d). Mode 4  $[t_3-t_4]$** 

After releasing the leakage energy, the primary current ( $i_{L1}$ ) and magnetizing current  $i_{lm}$  decays to zero at time  $t=t_4$ . Diode  $D_1$  is conducting .Fig.5. (d) Shows the equivalent circuit of the proposed converter in this mode. The leakage inductor energy can be recycled, and the voltage stress of the switch can be limited.

**(e). Mode 5  $[t_4-t_5]$** 

At  $t=t_4$ , the switch Q is turned on , and voltage across the switch  $V_{DS}$  reduces to zero. Diode  $D_2$  is still conducting and Diode  $D_1$  is turned off .The leakage inductor  $L_{K1}$  and  $L_m$  charged to input voltage ( $V_s$ ) and current starts to increases as shown in Fig.5.(e).

**B. Formula Derivation**

When the switch (Q) is turned on, the voltage across the magnetizing inductor ( $L_m$ ) and  $V_{L2}$  are written as

$$V_{lm} = V_s \quad (1)$$

$$V_{l2} = n V_{lm} = n V_s \quad (2)$$

When the switch (Q) is turned off, the voltage across the magnetizing inductor ( $L_m$ ) and  $V_{L2}$  are written as

$$V_{Lm} = -V_{C1} \quad (3)$$

$$V_{l2} = n V_{lm} = -n V_{C1} = V_{C2} + V_{C1} + V_s - V_o \quad (4)$$

$$V_{l2} = 2(V_{C1} + V_s) - V_o$$

Where the voltage across the capacitor ( $C_2$ ) can be written as

$$V_{C2} = V_{C1} + V_s \quad (5)$$

By using voltage-second balance principle on N1 and N2 of the coupled inductor , the following Equations are written as

$$\int_0^T V_s dt + \int_0^T -V_{C1} dt = 0 \quad (6)$$

$$\int_0^T n V_s dt + \int_0^T (2V_{C1} + V_s) - V_o dt = 0 \quad (7)$$

From equation (6) and (7),  $V_{C1}$  and  $V_o$  are derived as

$$V_{C1} = \frac{D}{1-D} V_s \quad (8)$$

$$V_o = \frac{(2+nD)}{1-D} V_s \quad (9)$$

As a result, the voltage gain of the step-up converter can be represented as

$$GV = \frac{V_o}{V_s} = \frac{(2+nD)}{1-D} \quad (10)$$

Equation (10) indicates that the converter accomplishes a high voltage gain by using voltage –lift technique and increasing the turn's ratio of the coupled inductor. Fig.6. Plots the ideal voltage gain against the duty ratio, under various turns ratios of the coupled Inductor.

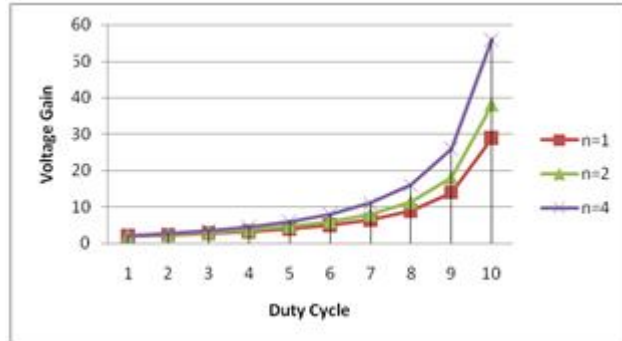


Figure 6. Voltage gain against duty ratio under various turns ratio of the coupled inductor

According to (8) and (9), the voltage stresses on the switch and the diodes are as follows

$$V_{DS} = V_{C1} + V_s = \frac{1}{1-D} V_s \quad (11)$$

$$V_{D1} = V_{C2} = V_{C1} + V_s = \frac{1}{1-D} V_s \quad (12)$$

$$V_{D2} = V_{C2} = V_{C1} + V_s = \frac{1}{1-D} V_s \quad (13)$$

$$V_{D0} = nV_s + V_o - V_{C2} = \frac{n+1}{1-D} V_s \quad (14)$$

From (9) and (11), the voltage stress of the main switch is clamped at a low voltage, and less than output voltage.

### III. DESIGN SPECIFICATIONS OF THE PROPOSED CONVERTER

A proposed converter had the following specifications:

1. Input DC voltage = 25V
2. Output DC Voltage = 240V
3. Switching Frequency = 50KHZ
4. Output power = 250W
5. Duty cycle = 65%

The on state resistance of the power switch and the primary winding of coupled inductor result much conduction loss for the low input power source of the proposed converter. Therefore, the maximum operating duty ratio is selected as a reasonable duty ratio for the high current issue in this design. The maximum duty ratio is selected nearly 0.65.

Based on above circuit specifications, the circuit design consideration can be described as below

#### A. Designing of Coupled Inductor

Here coupled inductor is modeled as a ideal transformer, the magnetizing inductor ( $L_m$ ) and a leakage inductor ( $L_k$ ). The turns ratio ( $n$ ) and the coupling coefficient ( $K$ ) of this

ideal transformer is defined as

$$n = \frac{n_1}{n_2} \quad (15)$$

$$K = \frac{L_m}{L_m + L_k} \quad (16)$$

Using above formula, “n” and “k” found to be 2 & 0.98 respectively, so chosen value of k=1 and using this values in the following equations

$$L_1 = \frac{nD(1-D)R}{2f(2+nD)} \quad (17)$$

$$\frac{L_1}{L_2} = \frac{N_2^2}{N_1^2} \quad (18)$$

$$L_m = \frac{D(1-D)^2 2R}{2(n+2)(2+nD)f} \quad (19)$$

From equation (17), (18) and (19) select the values  $L_1=79.28\mu H$ ,  $L_2=317\mu H$ , and  $L_m=13.87\mu H$ .

#### B. Designing of Capacitors

##### 1. Capacitor $C_1$ & $C_2$

Using the following equations,

$$C_1 = I_s \frac{(1-D)}{fV_s}$$

$$C_2 = I_o \frac{D(1-D)}{fV_s}$$

Select the value of capacitor  $C_1=2.6\mu F$ ,  $C_2=0.182\mu F$

##### 2. Filter Capacitor $C_o$

To find the value of filter capacitor “Co” for a desired output voltage ripple, we note that the capacitor resistor combination at the output of converter act as a low –pass filter for the current through the boost diode.

$$C_o = \frac{I_o(1-D)[V_o - V_s(2+nD)]}{2V_o fV_s}$$

Using this equation select Co is found to be  $51.70e^{-9}$  F

3. Based on above design analysis, voltage across the power switches and diodes are determined from equation (11) to (14). Accordingly the power MOSFET and diodes  $D_1$ ,  $D_2$  and  $D_o$  are selected respectively.

Fig.7. shows the Simulation diagram of proposed converter and Fig.8. Shows the simulation waveforms for  $P_o=250W$  and  $V_s=25$  V. The proposed converter is operated at CCM. The simulated waveforms agree with the steady state analysis circuit design. From Fig .8. (a) ,  $V_{DS}$  is clamped at approximately 60V during the switch off period. The voltage stress of the switch is effectively clamped without any snubber circuit. Therefore, a low –voltage rating power switch with a low on stage resistance for the high efficiency conversion of the proposed converter is adopted .Fig.8. (b) Shows the conduction of diode  $D_1$  and  $D_2$ .



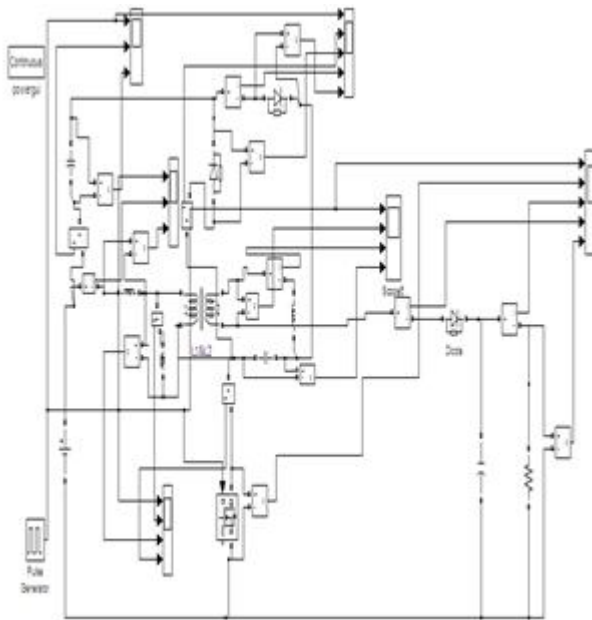


Figure 7. Simulation Diagram of Proposed Converter

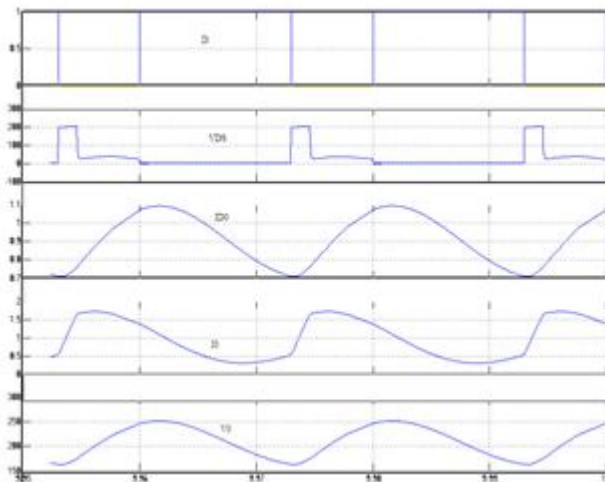
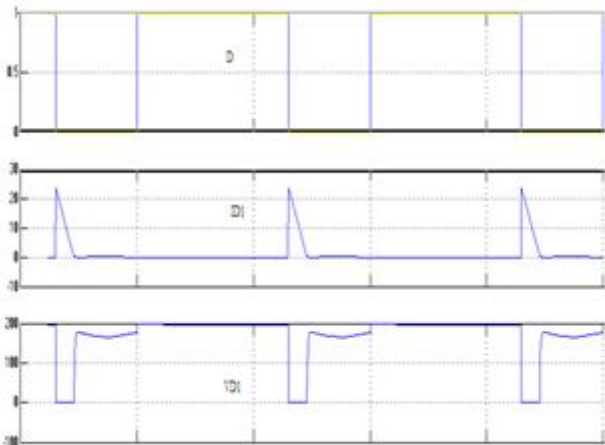
(a) proposed converter with  $V_o=250V$  and  $P_o=250W$ (b) Result of  $i_{D1}$ ,  $V_{D1}$ ,  $i_{D2}$  and  $V_{D2}$  of proposed converter

Fig.9. shows the experimental conversion efficiency of the proposed converter at condition  $D=0.65$ ,  $n=2$ . The maximum efficiency was around 96.96 % at  $P_o=240W$  and  $V_s=25V$ . The result verify that the proposed converter has

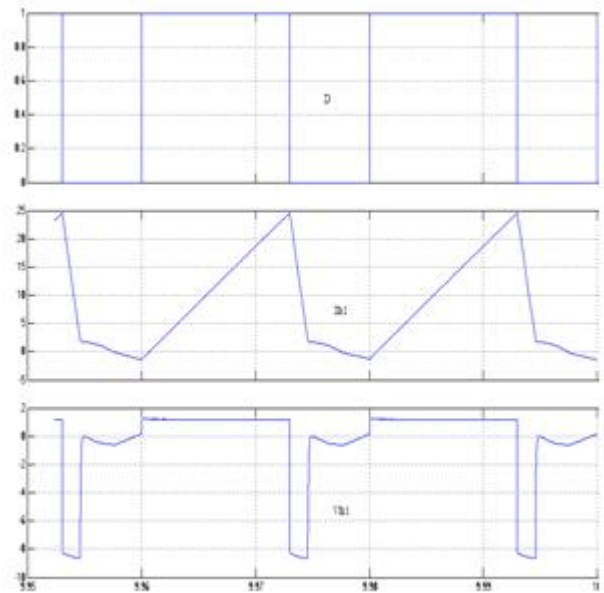
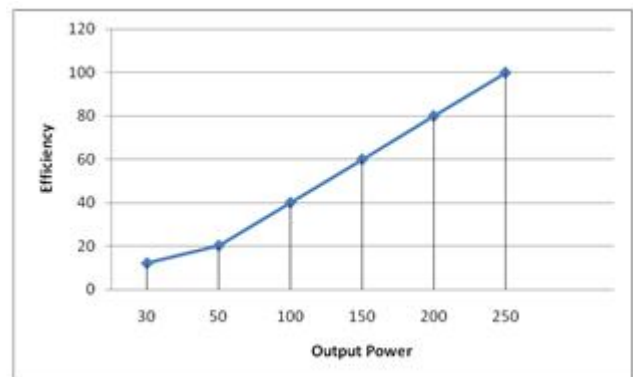
(c)  $i_{Lm}$  and  $V_{Lm}$  of proposed converterFigure 8. Simulation results for proposed converter under CCM for  $n=2$ 

Figure 9. Conversion efficiency of the proposed converter at different output powers

high-efficiency conversion, which is higher than conventional converters. Since the low input is applied in this energy conversion system, the input of proposed converter should suffer very high current which result much conduction loss during the switch on period. Thus, it will result in lower conversion efficiency. Furthermore, the proposed converter uses only one active switch for the energy conversion, which also suffers very current during the switch on period. Thus the proposed converter is suitable for low-middle power applications. In order to reduce the switch conduction loss, the switches in parallel are usually adopted for this high current issue to improve efficiency. This approach can also be used for the proposed converter in high power applications.

## CONCLUSION

This study has developed a high voltage gain Boost converter to achieve the High step-up voltage gain with voltage lift technique. The proposed converter has been highly efficient because it recycles the energy stored in leakage inductor of the coupled inductor while providing zero-voltage turn

ON of the main switch. Since voltage across the switch is clamped, the low-voltage rating and low-on-resistance power switch can be selected to improve efficiency. The operating principle and steady state analysis have been described in detail. The simulation results have indicated that the full load efficiency was 96.96% at  $V_s=25V$  at  $P_o=240W$ . Thus, the proposed converter is suitable for power conversion systems, such as fuel-cell-and solar-cell-based power conversion systems, high-intensity discharge lamps for automobiles head lamps etches authors can conclude on the topic discussed and proposed. Future enhancement can also be briefed here.

## REFERENCES

- [1] E. M. Fleming and I. A. Hiskens, "Dynamic of a microgrid supplied by solid oxide fuel cells," in *Proc. IEEE, IREP Sym.*, Aug. 2007, pp. 1–10.
- [2] A. Kwasinski and P. T. Krein, "A microgrid-based telecom power system using modular multiple-input DC–DC converters," in *Proc. IEEE Int. Telecommun. Energy Conf. (INTELEC)*, 2005, pp. 515–520.
- [3] J. M. Carrasco, L. G. Franquelo, J. T. Bialasiewicz, E. Galvan, R. C.P. Guisado, M. A. M. Prats, J. I. Leon, and N. Moreno-Alfonso, "Power electronic systems for the grid integration of renewable energy sources: A survey," *IEEE Trans. Power Electron.*, vol. 53, no. 4, pp. 1002–1016, AUGUST 2006.
- [4] N. Mohan, T. M. Undeland, and W. P. Robbins, *Power Electronics: Converters, Applications, and Design*. New York: Wiley, 1995.
- [5] Rong-Jong Wai, and Rou-Yong Duan, "High Step-Up Converter with Coupled Inductor" *IEEE Trans. On Power Electron.*, VOL. 20, NO. 5, SEPTEMBER 2005.
- [6] Rong-Jong Wai, Chung-You Lin, Rou-Yong Duan, and Yung-Ruei Chang, "High Efficiency DC-DC Converter with High Voltage Gain and Reduced Switch Stress" *IEEE Tran.on Industrial Electronics*, VOL.54, NO.1, FEBRUARY 2007
- [7] Tsai-Fu, Yu-Sheng Lai, Jin-Chyuan Hung, and Yaow-Ming Chen, "Boost Converter With Coupled Inductors and Buck-Boost Type of Active Clamp" *IEEE Tran.on Industrial Electronics*, VOL.55, NO.1, JANUARY 2008.
- [8] Jung-Min Kwon, and Bong-Hwon, "High Step-Up Active-Clamp Converter With Input-Current Doubler and Output-Voltage Doubler for Fuel Cell Power Systems" *IEEE Trans. Power Electron.*, vol. 24, no.1, JANUARY 2009.
- [9] Ching-Tsai Pan, and Ching-Ming Lai, "A High Efficiency High Step-Up Converter With Low Switch Stress for Fuel Cell System Applications" *IEEE Tran.on Industrial Electronics*, VOL.57, NO.6, JUNE 2010.
- [10] Shih-Kuen Changchien, Tsorng-Juu Liang, Jiann-Fuh Chen and Lung Sheng Yang "Novel High Step-Up DC-DC Converter for Fuel Cell Energy Conversion System" *IEEE Tran.on Industrial Electronics*, VOL.57, NO.6, JUNE 2010.
- [11] Hyun-Lark Do, "A Zero-Voltage-Switching DC–DC Converter With High Voltage Gain" *IEEE Trans. On Power Electron.*, VOL. 26, NO. 5, MAY 2011.
- [12] Shih-Ming Chen, Tsorng-Juu Liang, Lung-Sheng Yang, and Jiann-Fuh Chen, "A Cascaded High Step-Up DC–DC Converter with Single Switch for Microsource Applications" *IEEE Trans. On Power Electron.*, VOL. 26, NO. 4, APRIL 2011.
- [13] Yi-Ping Hsieh, Jiann-Fuh Chen, Tsorng-Juu Liang, and Lung-Sheng Yang, "A Novel High Step-Up DC–DC Converter for a Microgrid System" *IEEE Trans. On Power Electron.*, VOL. 26, NO. 4, APRIL 2011.
- [14] Hyun-Lark Do, "Nonisolated Bidirectional Zero-Voltage-Switching DC–DC Converter" *IEEE Trans. On Power Electron.*, VOL. 26, NO. 9, SEPTEMBER 2011.
- [15] Ahmad Mousavi, Pritam Das, and Gerry Moschopoulos, "A Comparative Study of a New ZCS DC–DC Full-Bridge Boost Converter With a ZVS Active-Clamp Converter" *IEEE Trans. On Power Electron.* VOL. 27, NO. 3, MARCH 2012.
- [16] Tsai-Fu Wu, Yong-Dong Chang, Chih-Hao Chang, and Jeng-Gung Yang, "Soft-Switching Boost Converter With a Flyback Snubber for High Power Applications" *IEEE Trans. On Power Electron.* VOL. 27, NO. 3 MARCH 2012.
- [17] Giorgio Spiazzi, Paolo Mattavelli, and Alessandro Costabeber, "High Step-Up Ratio Flyback Converter With Active Clamp and Voltage Multiplier" *IEEE Trans. On Power Electron.*, VOL. 26, NO. 11, NOVEMBER 2011.
- [18] Yi-Ping Hsieh, Jiann-Fuh Chen, Tsorng-Juu (Peter) Liang, and Lung-Sheng Yang, "Novel High Step-Up DC–DC Converter With Coupled-Inductor and Switched-Capacitor Techniques for a Sustainable Energy System" *IEEE Trans. On Power Electron.* VOL. 26, NO. 12, DECEMBER 2011